The kSZ effect as a test of general radial inhomogeneity in LTB cosmology

Philip Bull,[*] Timothy Clifton,[†] and Pedro G. Ferreira.[‡]

Department of Astrophysics, University of Oxford, OX1 3RH, UK.

(Dated: November 15, 2011)

The apparent accelerating expansion of the Universe, determined from observations of distant supernovae, and often taken to imply the existence of dark energy, may alternatively be explained by the effects of a giant underdense void if we relax the assumption of homogeneity on large scales. Recent studies have made use of the spherically-symmetric, radially-inhomogeneous Lemaître-Tolman-Bondi (LTB) models to derive strong constraints on this scenario, particularly from observations of the kinematic Sunyaev-Zel'dovich (kSZ) effect which is sensitive to large scale inhomogeneity. However, most of these previous studies explicitly set the LTB 'bang time' function to be constant, neglecting an important freedom of the general solutions. Here we examine these models in full generality by relaxing this assumption. We find that although the extra freedom allowed by varying the bang time is sufficient to account for some observables individually, it is not enough to simultaneously explain the supernovae observations, the small-angle CMB, the local Hubble rate, and the kSZ effect. This set of observables is strongly constraining, and effectively rules out simple LTB models as an explanation of dark energy.

I. INTRODUCTION

Observations of distant type-Ia supernovae are often taken to imply that the Universe has entered a phase of accelerating expansion, and may therefore contain 'dark energy' [1, 2]. Such a conclusion, however, cannot be inferred from the supernova data alone – a model of the Universe is also required. At present, the simplest and most widely applied cosmological models are based on the Friedmann-Lemaître-Robertson-Walker (FLRW) solutions of general relativity. These solutions are highly symmetric, and determining their validity as models of the real Universe is of critical importance for determining the veracity of the claims involving dark energy. It is toward these ends that this study is aimed: Are spatially homogeneous and isotropic models with dark energy the only ones capable of accounting for the recent cosmological observations that appear to imply acceleration?

The inference of acceleration is of profound consequence, not just for cosmology and gravitational physics, but also for particle and high energy physics. An accelerating Universe has an entirely different causal structure from one that is decelerating, with the vacuum itself taking on a non-zero energy density and becoming thermal. Beyond this there is the 'cosmological constant problem', that contributions from the zero-point energy of quantum fields, and any bare cosmological term in Einstein's equations, must cancel up to 1 part in 10^{120} [3]. Such incredible fine-tuning is widely believed to signify nothing less than a crisis in modern physics, and so the task of verifying the assumptions that go into our cosmological models becomes one of the utmost importance.

Here we focus on the problem of radial inhomogeneity, as modeled by the Lemaître-Tolman-Bondi (LTB) solutions of general relativity [4–6]. These are the general spherically-symmetric solutions of Einstein's equations with dust. They are widely known to have more than enough freedom to account for the supernova observations without recourse to dark energy [7], and are often referred to as 'void models' in the literature (but see also [8]). The relevant question is then whether or not these models are compatible with other observational probes of cosmology.

This question has been addressed by various authors in a number of different contexts [9–21]. Most of these studies have, however, limited themselves to the special case of space-times that have a spatially homogeneous energy density at early times. This is achieved by considering only those models that have a constant 'bang time'. In this case it is known that while the small angle CMB generated by a power-law spectrum of initial fluctuations can be easily reproduced within void models, an unacceptably low value of H_0 is required to do so [20, 21]. However, it is also known that this problem can be alleviated by allowing for *general* radial inhomogeneity, with non-constant bang time [20]. Here we address the problem of whether or not other cosmological observables are also consistent with models that allow for this additional freedom, as well as further investigating the parameter space of solutions that fit the small-angle CMB.

We will be interested in particular in the kinematic Sunyaev-Zel'dovich (kSZ) effect [22]. This effect is due to the inverse Compton scattering of photons from the Cosmic Microwave Background (CMB) off of electrons in distant clusters of galaxies. The rescattered light can be collected by observers who are looking at the cluster. If in the rest frame of the electrons the CMB has a non-zero dipole moment (in the direction of the observer) then the reflected light that the observer sees has its spectrum shifted. Such shifts are expected to be observable by upcoming experiments, and although they have yet to be directly detected [62], constraints have already been

---

[*]Electronic address: Phil.Bull@astro.ox.ac.uk
[†]Electronic address: Tim.Clifton@astro.ox.ac.uk
[‡]Electronic address: P.Ferreira1@physics.ox.ac.uk

placed on the allowed magnitude of this effect [23–27].

The kSZ effect is a particularly powerful probe of inhomogeneity as it allows us to make observations not only along the null cone that is the boundary of our causal past, but also along null curves that go inside this cone. The distant galaxy clusters essentially act as mirrors, reflecting light from the last scattering surface that would otherwise be unobservable to us. This extra information is above and beyond that which is available from the usual observations of distance measures, expansion rates and number counts, and so it is of great potential significance as a cosmological probe. The power of the kSZ effect in this context appears to have first been pointed out by Goodman in [28], although the first application of it to models that attempt to account for dark energy was performed by García-Bellido and Haugbølle [29]. These authors considered models with constant bang time only. We build on their work by allowing for a radially dependent bang time.

To make progress it will be necessary to make a number of assumptions, which to avoid confusion we will state here. We assume the following:

- That there is perfect spherical symmetry, with ourselves at the center of symmetry.

- That the formation of the last scattering surface proceeds as in FLRW cosmology.

- That there is a constant ratio of photons to baryons in the early universe.

- That the spectrum of initial fluctuations is a power law in wave number, k.

- That the energy density and all functions in the metric have smooth profiles.

The first of these is inherent in the problem we have chosen to address. General perturbations to this exact set of symmetries have been considered in [30] and [53], and the effects of being off-center have been considered in [19]. The second of these points is made for convenience. To date, we are unaware of any rigorous calculation involving the formation of the last scattering surface in inhomogeneous space-times. The effect of allowing for an inhomogeneous photon-to-baryon ratio has been considered in [31], and the related question of changing the position of the last scattering surface, while keeping the bang time constant, has been addressed in [18]. The effect of allowing a kink in the spectrum of initial fluctuations has been considered in [32]. We will not consider these freedoms further here, but note that a constant bang time is an assumption that would be added to similar lists in most other papers. For details of the effects of relaxing these assumptions, we refer the reader to the papers cited above.

In Section II we present the LTB solutions, and discuss how distance measures and redshifts are calculated within them. We then discuss the effects of the two radial degrees of freedom in these solutions, one of which is the bang time. In Section III we discuss some of the cosmological probes that can be applied to these models, with particular reference to the kSZ effect. We also discuss why these observations are problematic for LTB models with constant bang time. In Section IV we present our results, which include a detailed investigation of the effect of a radially varying bang time on CMB and H_0 observations, as well as the kSZ effect. We show that, despite the additional freedom in the bang time, there is a combination of key observables that cannot be fitted simultaneously. We conclude in Section V that this effectively rules out void models as an explanation of dark energy, unless one is prepared to discard one or more of the assumptions that we have listed above.

II. THE MODEL

In order to model general radial inhomogeneity we will use the Lemaître-Tolman-Bondi (LTB) solutions of general relativity. These are given by the line-element [4–6]

$$ds^2 = dt^2 - \frac{a_2^2(t,r)}{1 - k(r)r^2}dr^2 - a_1^2(t,r)r^2d\Omega^2, \quad (1)$$

where $a_2 = (a_1 r)'$, and where a_1 must satisfy

$$\left(\frac{\dot{a}_1}{a_1}\right)^2 = \frac{8\pi G}{3}\frac{m(r)}{a_1^3} - \frac{k(r)}{a_1^2}. \quad (2)$$

The functions $k(r)$ and $m(r)$ are arbitrary functions of the radial coordinate, and primes and over-dots denote partial derivatives with respect to r and t, respectively. These solutions are exact, and are the general spherically symmetric dust-only solutions to Einstein's equations. They admit a three dimensional group of Killing vectors that act transitively on the surfaces of constant r and t, and are spatially isotropic about the origin only.

Solutions to Eq. (2) are of the form $a_1 = a_1(r, t - t_B(r))$, which introduces a third arbitrary function of r. This gives a total of three free functions: $k(r)$, $m(r)$, and $t_B(r)$. We refer to these quantities as the spatial curvature, gravitational mass density (distinct from the local energy density) and bang time, respectively. In the limit of homogeneity they are all constant. It can also be seen that one can perform a coordinate transformation $r \to f(r)$ that preserves the form of the metric in Eq. (1). This freedom can be used to set $m =$ constant, without loss of generality (assuming $(mr^3)'$ is always positive). This leaves us with the general solution in terms of the spatial curvature, $k(r)$, and bang time function, $t_B(r)$, only. Analytic parametric solutions to Eq. (2) are known, and can be found in [33].

We can now use these solutions as cosmological models that exhibit an arbitrary amount of radial inhomogeneity by supposing ourselves to be observers at the center of symmetry. Such models are known to be able to produce excellent fits to the supernova data without requiring any

dark energy, and often result in the observer being at the center of gigaparsec-scale underdensity, or 'void'. This is possible due to both temporal *and* spatial variations in the geometry of the space-time that are experienced by photons as they travel through the void. Such calculations require knowledge of redshifts and distance measures in this space-time, which we will now consider.

Let us first define two different Hubble rates: a transverse one, $H_1 \equiv \dot{a}_1/a_1$, and a radial one, $H_2 \equiv \dot{a}_2/a_2$. In the limit of homogeneity these two quantities are identical, but differ, in general, in inhomogeneous space-times. The redshift of photons traveling along radial geodesics can then be calculated by integrating the radial Hubble rate as follows:

$$1 + z = \exp\left\{ \int_{t_e}^{t_o} H_2(t, r(t)) dt \right\}, \qquad (3)$$

where $r = r(t)$ is a solution of the radial geodesic equation, and t_e and t_o are the time at which the photon was emitted and observed, respectively. Note that the relation $(1 + z) \propto 1/a_1$ no longer holds, in general. We can also calculate the angular diameter distance to objects at redshift z using

$$d_A(z) = r(z)\, a_1(r(z), t(z)), \qquad (4)$$

where $t(z)$ is calculated by inverting $z = z(t)$ from Eq. (3), and $r(z) = r(t(z))$ is found using the radial null geodesic equation. Luminosity distances are then given by Etherington's reciprocity theorem [34]

$$d_L(z) = (1 + z)^2 d_A(z), \qquad (5)$$

which is true in any space-time. The local energy density is given by $\rho = (mr^3)'/3a_2 a_1^2 r^2$.

In this paper we will often choose to parametrize the two functions $k(r)$ and $t_B(r)$ as Gaussian curves, with

$$k(r) = A_k \exp(-r^2/\lambda_k^2) + k_\infty \qquad (6)$$
$$t_B(r) = A_{t_B} \exp(-r^2/\lambda_{t_B}^2) f(r), \qquad (7)$$

where A_k, A_{t_B}, λ_k, λ_{t_B} and k_∞ are constants, and the factor $f(r) = \exp(-r^{10}/\lambda_{t_B}^{10})$ is included to attenuate the bang time profile at large r. This is done so that wide profiles can be used, while limiting the effect of early inhomogeneity on the central observer's last scattering surface, and is discussed further in Section II B. The profiles above are defined by their amplitudes, A_i, and widths, λ_i. A further parameter k_∞ defines the asymptotic spatial curvature, outside the void. The timescale of the model is set by choosing a local Hubble parameter $H_0 = H_1|_{r=0} = H_2|_{r=0}$ at time t_o, where $(t_o - t_B)|_{r=0}$ is the age of the Universe along the worldline of an observer at $r = 0$. A rescaling can be used to set $a_1(0, t_o) = a_2(0, t_o) = 1$.

The amplitudes in Eq. (6) and (7) can be expressed in a more familiar form as fractions of the total density at the origin today. For this purpose let us define

$$\Omega_{k_1} \equiv -A_k/H_0^2 \qquad (8)$$
$$\Omega_{k_2} \equiv -k_\infty/H_0^2 \qquad (9)$$
$$\Omega_k \equiv \Omega_{k_1} + \Omega_{k_2} \qquad (10)$$
$$\Omega_m \equiv \frac{8\pi G}{3H_0^2} m(r), \qquad (11)$$

such that $\Omega_k + \Omega_m = 1$. Furthermore, restricting ourselves to $\Omega_m \geq 0$ means that we consider only $\Omega_k \leq 1$.

Let us now briefly consider the consequences of fluctuations in $k(r)$ and $t_B(r)$. The former of these is the analog of the spatial curvature in FLRW solutions, which dominates the dynamical evolution of the Universe at late times. The latter changes the location of the initial singularity, and so can be thought of modifying the early stages of the Universe's history. This interpretation is supported by treating the LTB geometry as a fluctuation about an FLRW solution. In this case the fluctuations in $k(r)$ can be mapped into growing modes, while fluctuations in $t_B(r)$ are mapped onto decaying modes [35].

A. An Inhomogeneous Late Universe

Let us first consider $k(r)$. It can be seen from Eq. (2) that $k < 0$ gives a positive contribution to the expansion of a_1, while $k > 0$ gives a negative contribution. This is the behavior we are familiar with from the Friedmann equation of FLRW cosmology. Unlike the homogeneous FLRW solutions, however, the expansion of a_2 does not always get a positive contribution from $k < 0$. On the contrary, in regions of $k < 0$ the expansion of a_2 can slow, and recollapse can occur. This behavior is well known, and can lead to the formation of a 'shell crossing singularity' when the collapsing region reaches $a_2 = 0$.

One can avoid shell crossing singularities in a region by satisfying the Hellaby-Lake conditions [36]. These depend on the sign of $k(r)$, and for $k \leq 0$ may be written using our notation as [37]

$$(mr^3)' \geq 0, \; t_B' \leq 0, \; \text{and} \; (kr^2)' \leq 0, \qquad (12)$$

while for $k > 0$ the last of these should be replaced by

$$\left[\log\left(\frac{m}{k^{\frac{3}{2}}} \right) \right]' + \frac{3t_B'|k|}{8\pi Gm} \geq 0. \qquad (13)$$

These conditions guarantee that $a_2 > 0$, so that shell crossing singularities cannot occur [63]. They are, however, very restrictive, and most applications of the LTB solutions to cosmology simply avoid the issue by making sure that shell crossings only happen in the distant future. They can then be considered as a breakdown of the model at some future time, after which a more sophisticated solution including pressure would be required to avoid the formation of singularities. The existence of pressure is expected to prevent the complete collapse of matter, and a large overdensity of collapsed structures is thus expected to form instead.

B. An Inhomogeneous Big Bang

Let us now consider the consequences of fluctuations in $t_B(r)$. If $t_B(r)$ is not constant, then the 'age of the universe' differs from place to place. This is a significant departure from the standard picture of the big bang, and may initially seem odd. Certainly, there have been a number of objections to allowing inhomogeneous bang times in the literature, with the result that to date most studies of void models have expressly set $t_B(r) =$constant *a fortiori*. In this section we will discuss the physical significance of an inhomogeneous big bang, and argue that it is reasonable to consider models with such a feature.

As mentioned above, fluctuations in $t_B(r)$ correspond to decaying modes when the space-time is approximated as a perturbed FLRW solution. A non-constant bang time therefore corresponds to an inhomogeneous early universe, and as one goes further back in time the size of the consequent inhomogeneity generally increases. As with the case of fluctuations in $k(r)$, there exist points beyond which the scale factor a_2 is contracting rather than expanding, and in cases where the Hellaby-Lake conditions are violated, shell crossing singularities can occur. In the case of fluctuations in $t_B(r)$, however, this behavior occurs at very early times rather than at very late times.

In Fig. 1 we illustrate the existence of surfaces of $a_2 = 0$ in cases with $t'_B > 0$, and regions with $H_2 < 0$ in cases with $t'_B < 0$. The former of these are the early universe analogue of the shell crossing singularities we described in the previous section, and in this case we consider the singular surface with $a_2 = 0$ to be our initial hypersurface. The latter case corresponds to regions that have started to collapse, but reach the singular surface $t = t_B$ before shell crossings occur. Contraction of this type should be expected to cause blueshifts when looking along exactly radial geodesics [38], and again this behavior has an analog in the inhomogeneities that form at late times [9, 17]. Such blueshifts would have profound effects if they were allowed to occur between the last scattering surface and an observer (for example, a distance-redshift relation $r(z)$ that is not monotonic could occur).

Célérier *et al.* [8] found that small variations in the bang time, of order hundreds of years, lead to temperature anisotropies in the CMB of $\mathcal{O}(10^{-6})$, which are currently only marginally too small to be observed. Larger bang time variations would have a stronger observational signal, but this need not be an issue if the region of varying bang time occurs far inside the void, away from the surface of last scattering that we see directly. Nevertheless, observers elsewhere in the space-time would see considerable anisotropies in their CMB sky, and this could be observable in the kSZ effect we see from CMB photons that rescatter off their cluster. The kSZ effect therefore has the potential to provide powerful constraints on the inhomogeneities caused by bang time fluctuations.

Of course, LTB models are dust-only solutions of Einstein's equations, and lose their validity when radiation
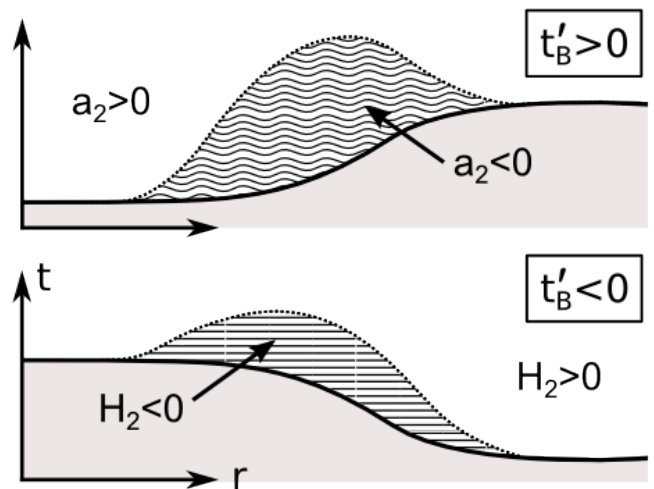

FIG. 1: Upper panel: If $t'_B > 0$ then a surface exists with $a_2 = 0$, corresponding to the occurrence of a shell crossing singularity (dotted line). Beyond this, the formal solution for the energy density gives negative values (hatched area). Lower panel: If $t'_B < 0$, regions with $H_2 < 0$ form (hatched area). The solid lines correspond to the surfaces $t = t_B$.

becomes important at early times [8, 31]. The introduction of a radiation fluid into inhomogeneous solutions complicates matters considerably, and we do not attempt to include the gravitational effects of radiation in our models here. However, in the same way that one would expect pressure to prevent the formation of shell crossing singularities at late times, one could reasonably speculate on a similar mechanism occurring at early times. In the present study we concentrate on the matter dominated phase of the Universe's history, which should be sufficient to model the Universe from last scattering to the present time. This is well modeled by the LTB solutions. We leave the consideration of the gravitational effects of inhomogeneous radiation fields to other studies. For further details of this the reader is referred to [31, 60].

An obvious concern with models of this type is that they are difficult to reconcile with early universe inflation. This is true with models that have $t_B =$constant, as well as models with an inhomogeneous big bang. One must then either discard inflation for the time being, or attempt to construct inflationary scenarios that result in occasional large inhomogeneities (see, e.g., [39] and [40]). Here we address the problem of what can be said about the geometry of the Universe directly from observations, rather than imposing requirements from theories of the very early universe.

III. OBSERVATIONAL PROBES, AND RESULTS WITH CONSTANT BANG TIME

Void models that reproduce the observed supernova distance modulus curve have proved relatively easy to

construct, and little more than a moderately deep underdensity with a comoving width of order a gigaparsec is required to obtain a satisfactory fit. Indeed, the ease with which the supernova observations can be reproduced has been one of the principle factors motivating interest in these models.

The introduction of such a large inhomogeneity, however, can hardly be expected to leave predictions for other cosmological observables unchanged, and so there have been a number of attempts to make detailed tests of voids using multiple data sets [9, 13, 21]. While thorough, these previous studies have limited themselves to the case of voids with constant bang times. In this section we summarize the constraints that can be imposed on such void models from observations of supernovae, the CMB, the local Hubble parameter, and the kSZ effect. In particular, we draw attention to the difficulty that voids with constant bang time have in fitting the CMB and H_0 simultaneously, and discuss the power of the kSZ effect as a test of large-scale inhomogeneity in these models [15, 16, 29].

In Section IV we will proceed to consider more general voids with varying bang times. This additional freedom allows some of the constraints on the specific observables discussed in this section to be weakened significantly (although a combined fit to all data sets remains elusive).

A. Supernovae

As noted above, fitting the supernova data is a relatively simple matter, and void models can be constructed that fit any given $d_L(z)$ curve *exactly* [41]. One should be aware, however, that reproducing the precise effects of Λ at low z requires an energy density profile that is 'cusped' at the center [12, 42]. Generic smooth profiles produce qualitatively different behavior, due to the Milne-like geometry near the origin, but can still be shown to be consistent with current data sets [12, 42].

B. The CMB and H_0

If the last scattering surface we observe is located in a region of the Universe that is homogeneous and isotropic enough to be modeled as being approximately FLRW then we can use standard techniques to calculate the power spectrum of fluctuations on that surface. The CMB that we measure on our sky then depends on the initial spectrum, which can be calculated using an effective FLRW model, and the projection of fluctuations from the last scattering surface onto our sky. This projection depends on the space-time geometry between us and the last scattering surface, and can be calculated from the angular diameter distance in Eq. (4). It is in this way that the CMB provides constraints on the geometry of the late Universe.

In general, voids and FLRW models with the same local geometry have different angular diameter distances to the last scattering surface, resulting in a relative shift in their observed CMB power spectra. Now, the distance to last scattering can be adjusted by changing the width and depth of the void, but this typically produces relatively small shifts that are not enough to bring the peak positions of the CMB power spectrum in line with current observational constraints [20]. Changing the curvature of the FLRW region near the last scattering surface, however, produces much larger effects [20], and good fits to the small-scale CMB power spectrum can be found for void models that have positive asymptotic curvature. Such models, however, require an anomalously low local Hubble rate ($H_0 \lesssim 50$ km s^{-1} Mpc^{-1}) in order to keep the expansion rate at last scattering low enough to be consistent with the data [20, 21]. This is strongly inconsistent with the observed value of $H_0 = 73.8 \pm 2.4$ km s^{-1} Mpc^{-1} recently found in [43]. The CMB+H_0 by themselves are therefore sufficient to effectively rule out simple void models with constant bang time.

One can attempt to avoid this conclusion by violating the assumptions that we set out in Section I. In particular, models with inhomogeneous last scattering surfaces have been considered in [14] and [31], and a non-power law spectrum of initial fluctuations has been considered in [32]. If one is prepared to consider such additional freedoms then the CMB+H_0 constraints can be considerably weakened.

In Section IV we will consider the consequences of CMB observations in general void models, where the bang time is allowed to vary. It has already been shown in [20] that the available constraints from the CMB+H_0 can be considerably weakened in this case, without any need to violate the assumptions introduced in Section I. In Section IV we will quantify this result, finding best fit models and confidence regions in parameter space. We will show that the best fit models have bang time fluctuations of order a billion years.

C. The kSZ Effect

A promising observable for testing large-scale homogeneity is the kinematic Sunyaev-Zel'dovich (kSZ) effect. This effect occurs because galaxy clusters contain hot gas that can Compton scatter CMB photons, leading to a frequency-dependent temperature increment/decrement of the CMB along the line of sight to the cluster. Such scattering events cause two separate effects that can be distinguished in the reflected light. The first is due to transfer of thermal energy from the cluster gas to the photons, and is known as the thermal Sunyaev-Zel'dovich effect. The second is due to the dipole, $\Delta T/T$, of the CMB radiation on the sky of an observer comoving with the reflecting cluster, and is known as the kinematic Sunyaev-Zel'dovich effect [22]. It produces a temperature change of $\Delta T/T$ in the reflected light, and is similar to the rel-

ativistic Doppler shift that one would experience by reflecting a beam of light off of a moving mirror.

As noted by Goodman [28], and explicitly calculated by García-Bellido and Haugbølle [29], observers who are off-center in a radially-inhomogeneous universe should expect to see a large $\Delta T/T$ in their CMB if they are comoving with the dust. This is because the distance-redshift relation becomes a function of direction in an inhomogeneous space-time, so that the surface of last scattering will appear to be at different distances/redshifts in different directions on the sky of an off-center observer. The result of a large kSZ effect then follows because most observers in the space-time see a highly anisotropic CMB. Of course, this is not the case in an FLRW universe, where one should anticipate a low kSZ signal due only to the peculiar motion of clusters. It is for this reason that the kSZ effect is expected to be a powerful probe of large-scale inhomogeneity.

In a void model the dipole in the CMB is aligned in the radial direction due to spherical symmetry, and can be calculated from the relative velocity to an observer at the same point who would see an isotropic CMB. It is this dipole that can then, in principle, be measured using the kSZ effect. Now, the magnitude of dipole, $\Delta T/T$, can be calculated for a given void model by finding the redshifts to last scattering when looking radially into and out of the void. The observer then sees an average temperature of $T = \frac{1}{2}(T_{in} + T_{out})$, where T_{in} and T_{out} are the temperatures of CMB photons seen when looking into and out of the center of symmetry, respectively, and the relative velocity with respect to the CMB rest frame that causes this dipole is given by

$$\beta = \frac{\Delta T}{T} = \frac{z_{in} - z_{out}}{2 + z_{in} + z_{out}}, \qquad (14)$$

where z_{in} and z_{out} are the redshifts to last scattering in the directions toward and away from the center of the void, respectively. They can be calculated from Eq. (3), which is valid for off-center observers [44]. The kSZ effect can also be measured as a power spectrum using [15, 16]

$$\left.\frac{\Delta T(\hat{n})}{T}\right|_{kSZ} = \int_0^{z_*} \beta(z)\delta_e(\hat{n}, z)\frac{d\tau}{dz}dz, \qquad (15)$$

where $\Delta T(\hat{n})/T$ is the CMB anisotropy seen by an off-center observer in a direction $\hat{n}$, τ is the optical depth along the line of sight, δ_e is the density contrast of electrons, and z_* is the redshift to the last scattering surface.

One should note that the calculation described above over-estimates $\Delta T/T$ in the reflected light because the anisotropy seen by off-center observers will not be purely dipolar, especially far from the center of the void [19]. The dipole contribution, however, is the dominant one at low z, and so we expect the prescription outlined above to be accurate enough for our current purposes. Observations of individual clusters have yielded upper limits of $\Delta T/T \lesssim 2000$ kms^{-1} [29], and more recent observations from ACT and SPT have produced upper limits on the

kSZ power spectrum at $\ell = 3000$ of 8 μK^2 and 13 μK^2, respectively [26, 27]. This is consistent with the typical peculiar velocities expected in ΛCDM of $\sim$400 kms^{-1}, but is strongly inconsistent with any large void with constant bang time that obeys the assumptions made in Section I [29].

An example $\beta(z)$ profile that an observer at the center of a large void with constant bang time could infer from observations of the kSZ effect is shown in Figure 2. Although this is only one example, the enormous magnitude of the effect is a generic result for observers located at the center of such voids. This directly demonstrates the utility of the kSZ effect as a probe of inhomogeneity on large scales, and explains why current observational constraints on the kSZ effect by themselves are enough to rule out simple voids with constant bang time. In Section IV we consider the consequences of a varying bang time on observations of the kSZ effect, and show that there exist general giant void models that are consistent with constraints from current observations.
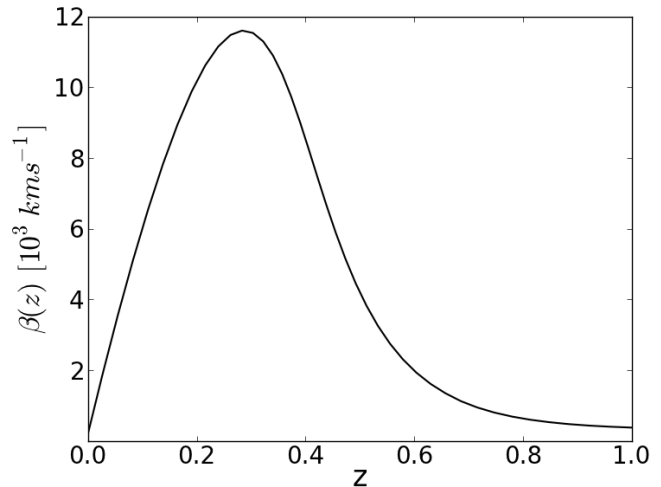

FIG. 2: An example of the relative velocity with respect to the CMB rest frame, $\beta(z)$, that would be inferred by a central observer in an example giant void with constant bang time.

D. Other Observables

So far we have discussed the specific observables of supernovae, the CMB+H_0, and the kSZ effect, and described how the latter two of these provide constraints on simple void models with a constant bang time that are sufficient to effectively rule them out. We have chosen to discuss these particular observables as we consider them to be reasonably well defined in void models, easily calculable, and very constraining. There are, of course, other observables that one could also consider. These include baryon acoustic oscillations (BAOs), galaxy correlation functions, and the integrated Sachs-Wolfe (ISW) effect,

to name just a few.

To understand these observables in the FLRW cosmological models one only needs linear perturbation theory about an FLRW background, which is very well understood. The observables in question can therefore be straightforwardly calculated. Linear perturbation theory in LTB cosmology, however, is significantly more complicated. In [30] a gauge invariant formalism for general perturbations in spherically symmetric space-times is applied to these models, and it is shown that scalar, vector and tensor modes no longer decouple. This means that complicated effects can occur that are not present in FLRW cosmology. The full consequences of this behavior have yet to be understood, and so here we avoid the use of observables that rely on linear perturbation theory. This includes BAOs, galaxy correlation functions and the ISW effect. For treatments of some of these observables when t_B =constant the reader is referred to [17].

IV. RESULTS WITH VARYING BANG TIME

In this section we examine the constraints that can be imposed on general void models in which the bang time is allowed to vary. This generalizes the previous results that were summarized in Section III.

As before, the observables we will use to constrain these models are the supernova distance moduli as functions of redshift, the CMB power spectrum on small scales, the local Hubble rate, and the kinematic Sunyaev-Zel'dovich effect. The specific data used for each observable will be explained in the subsections that follow. We use the parametrized LTB models of Section II, and a Metropolis-Hastings Markov chain Monte Carlo (MCMC) method to explore parameter space [64]. The likelihood function for each set of parameters is modeled as a chi-squared distribution, such that $-2\log\mathcal{L} \approx \chi^2$, and 'goodness of fit' is quantified by comparing to a ΛCDM model with $\Omega_\Lambda = 0.734$ and $h = 0.710$ [45].

We first proceed by considering each observable individually, and then go on to consider the constraints available from combinations of different observables. It is found that the additional freedom allowed by varying the bang time significantly weakens the constraints that each observable imposes by itself, but that the combined power of all observables is still enough to effectively rule out these models as a possible explanation of dark energy. In particular, we show that neither the CMB+H_0 observations, nor the upper bounds on the kSZ effect for individual clusters, have the ability to rule out these models by themselves, as is the case when the bang time is assumed to be constant.

A. Supernovae

In the fits that follow we use the Union2 compilation of 557 supernovae, which extends out to $z \sim 1.4$ [46].

Other supernova data sets also exist, and void fitting procedures are known to exhibit some sensitivity to the data set that is chosen [12, 32]. We choose the Union2 data as it is the most extensive catalog, and the most widely used in the literature. The absolute magnitude of the supernovae in the Union2 data set is an unknown parameter, and is therefore fitted to each model individually as a nuisance parameter. We use the published errors in this data set, which includes an 'intrinsic error' that is added to minimize the reduced χ^2 of ΛCDM. The full Union2 "covariance matrix with systematics" is used in performing all of the likelihood estimates that follow.

As with t_B =constant, there is no problem fitting the supernova data without dark energy.

B. The CMB and H_0

In FLRW cosmology, and for our current purposes, the CMB power spectrum can be efficiently specified on small scales with only three pieces of information [65]: (i) the acoustic horizon scale at decoupling, (ii) the acoustic scale at matter-radiation equality, and (iii) the projected scale of the CMB onto our sky. This information can be combined into three parameters in a number of different ways [31, 47–49], but here we choose to specify it as the 'shift parameter', S, the Hubble rate at last scattering, H_*, and the redshift of the last scattering surface, z_*. The shift parameter is defined as $S \equiv d_A(z_*)/\hat{d}_A(z_*)$, where $\hat{d}_A(z_*)$ is the angular diameter distance to the last scattering surface in a fiducial spatially flat FLRW model with $\Omega_m \simeq 1$. This quantity corresponds to the change in scale of fluctuations on the sky that two observers in different space-times would see when looking at two identical last scattering surfaces.
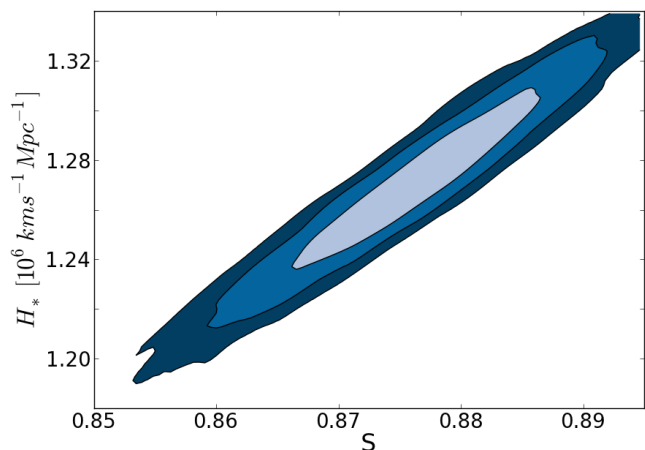

FIG. 3: Marginalized likelihood for the parameters S and H_*, found using WMAP 7-year data and a modified version of CosmoMC [51]. Shaded regions show the 68%, 95%, and 99.7% confidence regions.
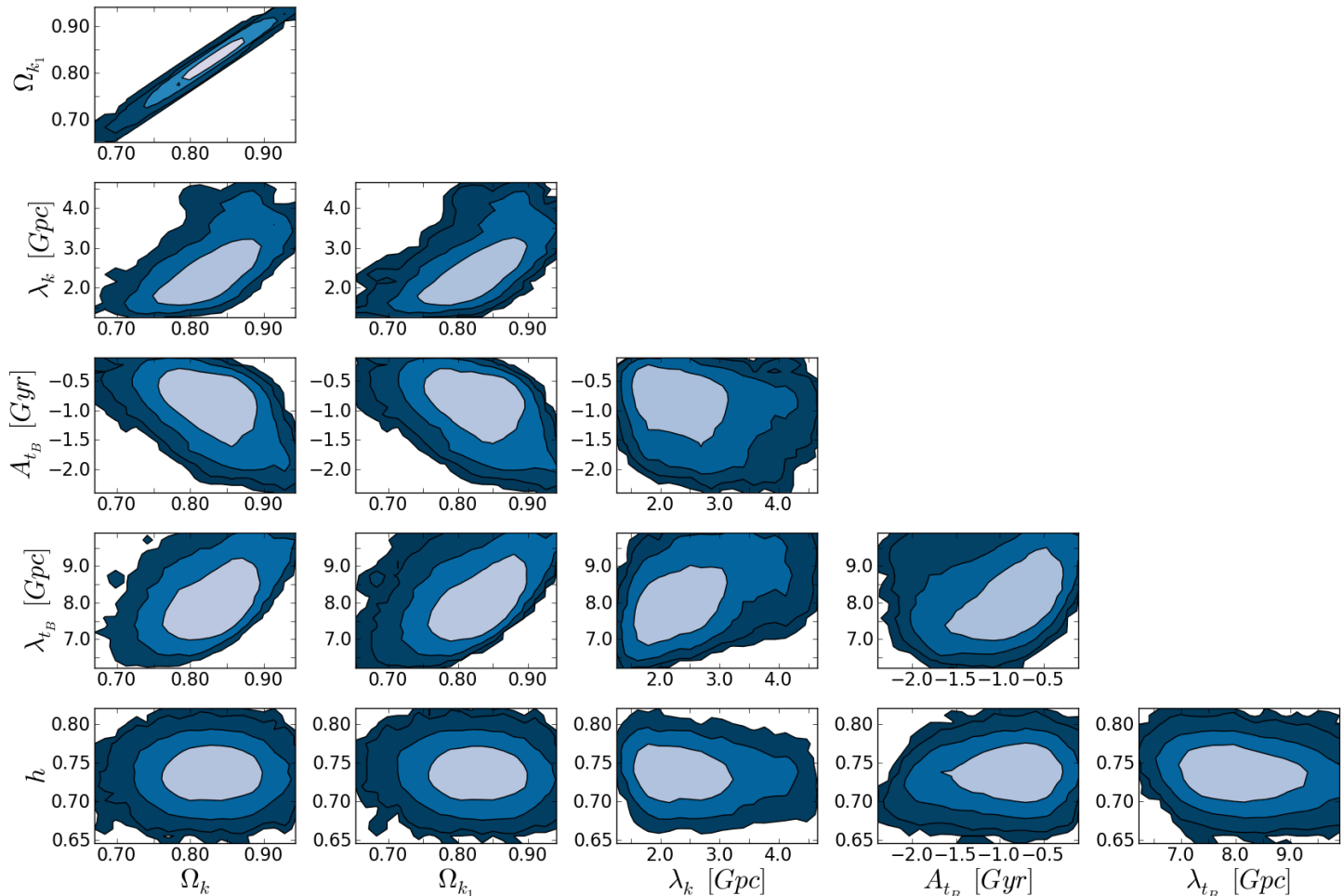
FIG. 4: Marginalized likelihoods for a Gaussian void model with varying bang time. Shaded regions show the 68%, 95%, and 99.7% confidence regions. Here we use $H_0 = 100h$ kms^{-1}Mpc^{-1}. See the text for other definitions.

Here, for simplicity, we take $z_* = 1090$, which is the redshift to the last scattering surface in ΛCDM and various other models [48] [66]. It now remains to impose constraints on S and H_*. To do this, we enforce the condition that the region of space in which the last scattering surface forms is well-approximated as being homogeneous and isotropic, so that standard results from FLRW cosmology can be applied in dealing with all of the physics up until the formation of the last scattering surface. We can then use CosmoMC [50] to calculate H_* and $d_A(z_*)$ for an observer in a spatially flat and dust dominated FLRW universe looking at this surface. Using the space-time geometry of our void models we can then calculate S and H_0 for an observer at the center of the void looking at an identical last scattering surface, with identical Hubble rate at last scattering, and at an identical redshift. This is the procedure followed in [20].

We use the WMAP 7-year data [51], with a modified version of CosmoMC, to constrain our models. In this analysis we choose to only use data at $\ell \geq 100$, as the low-ℓ power spectrum is dominated by the ISW effect

(see Section III D for a brief discussion of this). This choice weakens the constraints that can be achieved on the scalar spectral index of the initial power spectrum, n_s. Conservatively, we fix $n_s = 0.96$ here [67]. The constraints that can then be imposed on S and H_* are shown in Fig. 3. The best fit values are found to be $S \simeq 0.875$ and $H_* \simeq 1.27 \times 10^6$ kms^{-1}Mpc^{-1}. These values are consistent with those found in [20, 21]. Note that the CosmoMC CMB fits were not performed jointly with the void model MCMC; instead, they were run beforehand to get likelihoods for S and H_*, which we then used as priors for the void model MCMC.

As discussed in Section III B, it is possible to construct simple void models with $t_B =$constant that satisfy the constraints on S displayed in Fig. 3. This can be achieved by simply changing the spatial curvature of the model at large z [20]. The constraints on H_*, however, are more difficult to satisfy. For simple Gaussian voids with $t_B =$constant, under the assumptions described above, the WMAP 7-year data [51] and the Union2 supernova data set [46] are enough to show that

$H_0 \lesssim 40 \, \mathrm{kms}^{-1}\mathrm{Mpc}^{-1}$ is required, which is in strong disagreement with the value of $H_0 = 73.8 \pm 2.4 \, \mathrm{kms}^{-1}\mathrm{Mpc}^{-1}$ found by Riess *et al.* [43]. Allowing z_* to vary can increase the upper bound on H_0 by around $5 \, \mathrm{kms}^{-1}\mathrm{Mpc}^{-1}$, and changing the precise functional form of $k(r)$ can also marginally change H_0 (see [9, 17]). These are relatively small effects, however, and unless one is prepared to reject one or more of the assumptions given in Section I, models with $t_B =$ constant remain strongly inconsistent with recent measurements of H_0.

Allowing the bang time function to vary significantly improves the ability of void models to fit the CMB+H_0 data [20]. In Fig. 4 we show the likelihood plots for the parameters $(\Omega_k, \Omega_{k_1}, \lambda_k, A_{t_B}, \lambda_{t_B}, H_0)$, when constrained with the WMAP 7-year data [51], the Union2 data set [46], and the measurement of $H_0 = 73.8 \pm 2.4 \, \mathrm{kms}^{-1}\mathrm{Mpc}^{-1}$ [43]. Good fits to the data are obtained for models with a bang time fluctuation of width 8000 Mpc that makes the Universe about 800 million years older in the center than it is at large r. The curvature profile is narrower than this, with a width of 2500 Mpc, and a depth of $\Omega_k = 0.83$ at the center. The preferred spatial curvature at large radii is only $\Omega_{k,2} \sim +0.002$. It can be seen that in this case the model is able to produce an acceptably large value of H_0, with a best-fit value of $73.6 \, \mathrm{kms}^{-1}\mathrm{Mpc}^{-1}$. When compared to the best-fit ΛCDM model we find that ΛCDM is slightly preferred, with $\Delta\chi^2 = +4.5$ for 560 degrees of freedom. Most of this difference is due to the void model having a poorer fit to the supernova data, even though it over-fits H_0 and the CMB data. Voids with slightly more complicated spatial curvature profiles produce fits to the data that are at least as good as ΛCDM.

In the best fitting models the curvature profile, $k(r)$, is largely responsible for shaping the void at low redshift, with $z \lesssim 1$. In this region the bang time gradient is small, and so has little effect. In the region $1 \lesssim z \lesssim 2$ the curvature profile then flattens out and the bang time gradient begins to change rapidly. This produces large fluctuations in $H_2(z)$ along our past null cone, such that H_2 can take lower values at large z. The low value of H_* required at last scattering can then be simultaneously accommodated with a large value of H_0 locally. The difference in profile widths therefore helps to explain how it is that a good fit to the data can be achieved.

C. The kSZ Effect

Let us now consider the kSZ effect in void models with varying bang times. The void-induced dipole, $\Delta T/T$, can be calculated in an LTB model by following the procedure below:

1. On every point on our past null cone, solve the radial null geodesic equation for light rays traveling both into and out of the center of the void.

2. Calculate the redshift to the last scattering surface along these geodesics using Eq. (3).

3. Calculate the dipole, $\Delta T/T$, using Eq. (14). This can be converted into an effective velocity using $\beta = \Delta T/T$.

This procedure relies on knowing the location of the last scattering surface at different values of r. For models with a constant bang time, this surface occurs at a constant time, $t = t_{LS}$. In models with varying bang time, however, it will not occur as a hypersurface of constant t, as the presence of a bang time gradient changes the time evolution of the radial Hubble rate and density at a given r. We therefore approximate the location of the last scattering surface as a hypersurface of constant density, ρ, rather than time, t. The precise location of the last scattering surface will turn out to be important, and we will discuss the consequences of altering its position as we proceed.

We use the upper limits on $\beta = \Delta T/T$ that have been measured from nine individual clusters [23–25], as collected in [29]. These clusters span a redshift range of $0.18 \leq z \leq 0.55$. The data have asymmetric statistical errors, and are subject to large systematic errors of up to $\sim 750 \, \mathrm{kms}^{-1}$. For further explanation of the uncertainties in this data set the reader is referred to [29].

Void models with constant t_B have already been shown to be inconsistent with even this limited data set, as we discussed in Section III C [29]. Within this class of models, and subject to the assumptions outlined in Section I, the best fitting voids are those that are either very shallow ($\Omega_{k_1} \ll 1$) or very narrow ($\lambda_k \ll 1$ Gpc), with the latter of these possibilities only working because it restricts the inhomogeneity to redshifts at which there are currently no data. We find that the extra freedom afforded by allowing the bang time to vary relaxes these tight constraints, and admits the possibility of allowing $\beta(z)$ to be small even in regions of the Universe that are strongly inhomogeneous, with Ω_{k_1} as large as 0.85.

Fig. 5 shows an example of a large void with varying bang time that produces small enough $\beta(z)$ to be compatible with the data discussed above. A model with the same curvature profile, $k(r)$, but a constant bang time is also displayed. It can be seen that the additional freedom allowed by the varying bang time has a considerable impact on $\beta(z)$. The energy density profile for this model is also displayed in the figure. One should note, however, that the functional form of the bang time fluctuation required to produce this result is more complicated than the simple profile of Eq. 7. Instead, a sum of two (modified) Gaussian curves was used, of the form

$$t_B(r) = A_1 \exp\left(-\left[(r-r_1)^2/\lambda_1^2 + (r-r_1)^6/\lambda_1^6\right]\right) \quad (16)$$
$$+ A_2 \exp\left(-\left[(r-r_2)^2/\lambda_2^2 + (r-r_2)^6/\lambda_2^6\right]\right),$$

where $A_{1,2}$, $r_{1,2}$, and $\lambda_{1,2}$ are the amplitude, offset from the origin and width of the Gaussians respectively. Despite the greatly increased freedom in this bang time profile, we were unable to find a model consistent with
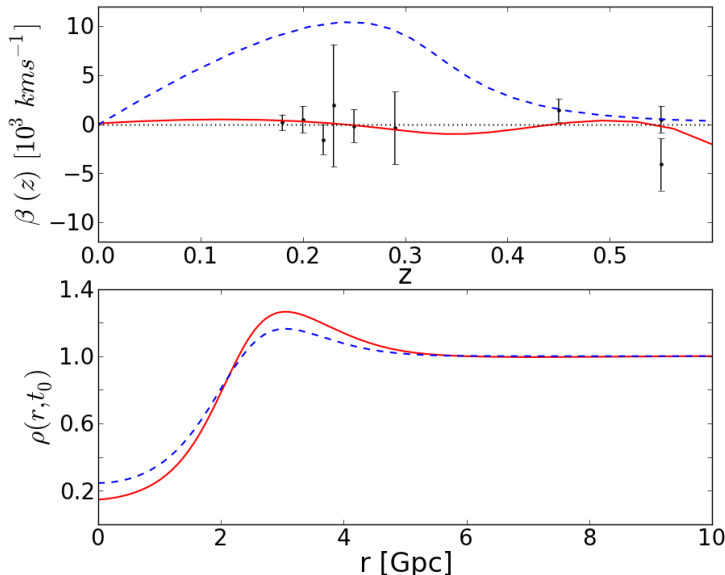
FIG. 5: Upper panel: Velocity with respect to the frame where the CMB is isotropic, $\beta(z)$, for models with constant bang time (dashed blue line) and non-constant bang time (solid red line). Both models have the same spatial curvature, $k(r)$. The data points are the upper limits for the nine clusters used in [29]. The solid red curve has a bang time fluctuation that is the sum of two Gaussians. Lower panel: Normalized density as a function of r on a hypersurface of constant t for the same two models.

the kSZ and supernova data simultaneously; the best-fit model had $\Delta\chi^2_{SN} = 44.1$ with ΛCDM. It is plausible that the situation could be improved by considering yet more complicated functional forms for $k(r)$ and $t_B(r)$, a possibility that we investigate in Section IV E. For simplicity, we have assumed in Fig. 5 that the offset caused by systematic errors in the data is zero. In reality, the data points would likely move slightly toward the curve to which they are being fitted, in order to improve the likelihood.

Finding models that agree with the upper limits on the statistical kSZ from ACT and SPT is a more difficult task. The kSZ power spectrum given by ΔT^2, in Eq. (15), depends on an integral of $\beta(z)$ over redshift. Deviations from $\beta = 0$ at any redshift therefore accumulate, potentially producing a large kSZ signal. It is possible that $\beta(z)$ could be made to change sign so that negative contributions cancel the positive ones, but this would require a delicate balancing of the competing effects to satisfy the statistical and single-cluster kSZ data simultaneously. One should bear in mind, however, that at large enough z, the effect of the void on the observed kSZ effect will decrease, as the angle subtended by the void on the distant observer's sky decreases, and the power in the dipole term of the anisotropy is shifted to higher multipoles [19].

In summary, we find that large void models with varying bang times may have enough extra freedom available to alleviate the constraints that can currently be imposed from observations of the kSZ effect. As we discuss in the following section, however, it is unlikely that after doing this there will be enough remaining freedom to accommodate any other observables.

D. Combined Constraints (SN+CMB+H_0+kSZ)

Let us now consider combining all of the observables we have discussed so far. These are the Union2 supernova data, the WMAP 7-year data, local measurements of H_0, and the kSZ effect.

In Fig. 6 we show the observed value of $\Delta T/T$ as a function of z that a central observer would measure from the kSZ effect in the models found in Section IV B. These models have been shown to provide good fits to the supernova data, and the CMB and H_0 data sets simultaneously. In Fig. 7 we show this information as a function of H_0 for redshifts $z = 0.05$, 0.10, 0.15, and 0.20. At all redshifts considered the distribution was bimodal, with some models having $\beta \approx 1$. Such incredibly high velocities are completely inconsistent with the data, and so here we show only the models with lower β. It can be seen that the value of the kSZ signal that one would observe from the center of these models is extremely large, even at low redshift. Such enormous kSZ signals are not compatible with the data displayed in Fig. 5, even with very large additional systematic uncertainties included.

The principal reason for this large effect appears to be the large width of bang time fluctuation that is favored by the combination of supernova, CMB and H_0 data sets (see Fig. 4). Because of this, observers at $z \gtrsim 0.1$ look through regions in which the bang time gradient is large when they look through the void. As discussed in Section II B, these regions host shell crossings when $t'_B > 0$. This pushes the surface of last scattering to much later times, and causes significant modifications to the redshift that this surface is seen at when looking through the center of the void. The redshift of the last scattering surface when looking away from the void experiences no such effect, as it is effectively fixed in position by the CMB data we see from the center. As a result, the values of z_{in} and z_{out} in Eq. 14 differ significantly, and the value of $\Delta T/T$ is therefore even larger than in the constant bang time case. Even at low z, this is unacceptably high.

E. More Complicated Profiles

One may now ask whether changing the specific forms of $t_B(r)$ and $k(r)$ that we have used so far affects our results. We showed in Section IV D that very poor agreement with the kSZ data is obtained for the models that best-fit the supernova, CMB, and H_0 data, but in Sec-
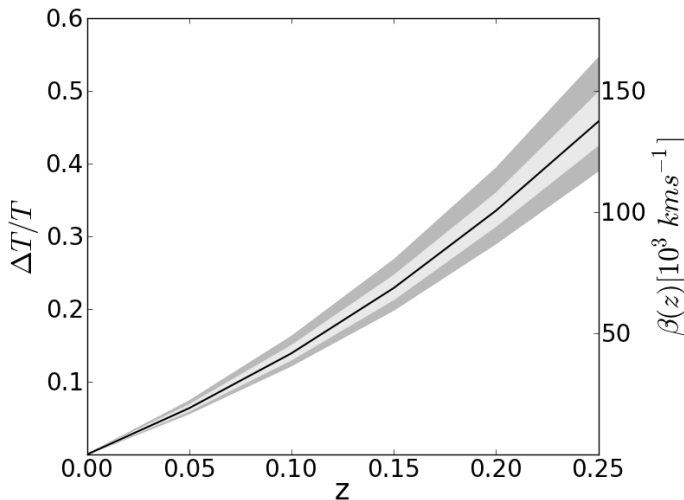
FIG. 6: The value of $\Delta T/T$ as a function of redshift for the best fitting models to the supernova, CMB and H_0 data sets, from Section IV B. The corresponding value of β is shown on the right-hand axis. The median and 68% and 95% confidence intervals are shown as the black line, and the light gray and dark gray bands, respectively. The actual distribution is bimodal, and here we show only the models with low $\Delta T/T$. Even for low redshifts, β is a large fraction of the speed of light.
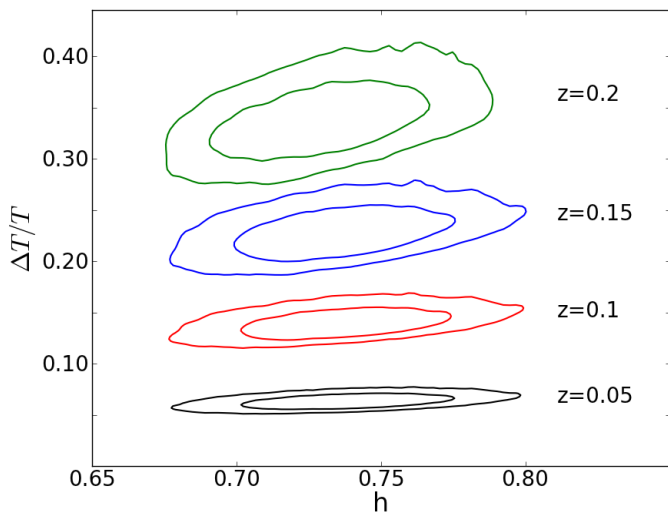

FIG. 7: The 68% and 95% likelihood contours in the space of $\Delta T/T$ and $H_0 = 100h$ kms^{-1}Mpc^{-1}, for off-center observers at $z = 0.05$, 0.10, 0.15 and $z = 0.20$, for the MCMC sample constrained by SN+CMB+H_0 data.

tion IV C we found that a good fit to the kSZ data could be obtained if a more complicated bang time profile was used. To see if a good fit to all of the observables is possible with a more complicated model, we ran an MCMC simulation using the spatial curvature profile of Eq. (6) and the extended bang time profile given by Eq. (16).

The MCMC was constrained by the supernova, CMB, H_0, and kSZ data simultaneously.

A plot of kSZ $\Delta T/T$ against H_0 for these models is shown in Fig. 8, and may be compared with Fig. 7. The models that maximize the likelihood have a $\beta(z)$ profile that is almost flat over the redshift range of interest (slightly larger at small z), and much less discrepant with the kSZ data. Relatively narrow spatial curvature and bang time profiles are preferred, extending out to only $z \sim 0.2$, and the bang time profiles are shifted towards the negative r direction (i.e. $r_{1,2} < 0$ in Eq. (16)). A preferred H_0 of only 44.0 kms^{-1}Mpc^{-1} is obtained, and the fit to supernova and CMB data is also poor; the best-fit model is inconsistent with the data, with $\Delta\chi^2 \approx 270$ compared to ΛCDM. We conclude that this is because the fit is most sensitive to the kSZ data; it is easy to find models that are wildly inconsistent with the kSZ data, as evidenced by Fig. 7, and so models that minimize the χ^2 with the kSZ data above all else are preferred. These tend to have low Hubble rates and narrow density profiles, features that are difficult to reconcile with the supernova and H_0 data. As such, it seems that even with the significantly more complex bang time profile, a good fit to all of the data simultaneously is not possible.

To further investigate the sensitivity of our results to the choice of profile parametrization, we now consider the model found by Célérier *et al.* in [8] that was constructed to reproduce the ΛCDM values of luminosity distance and Hubble rate as a function of redshift, but without dark energy. The density profile on a hypersurface of constant t takes the form of a "hump" in this model, rather than a void, and the bang time gradient at low z is negative, so there are no shell crossings at early times. Instead, this model has double-valued redshifts at high
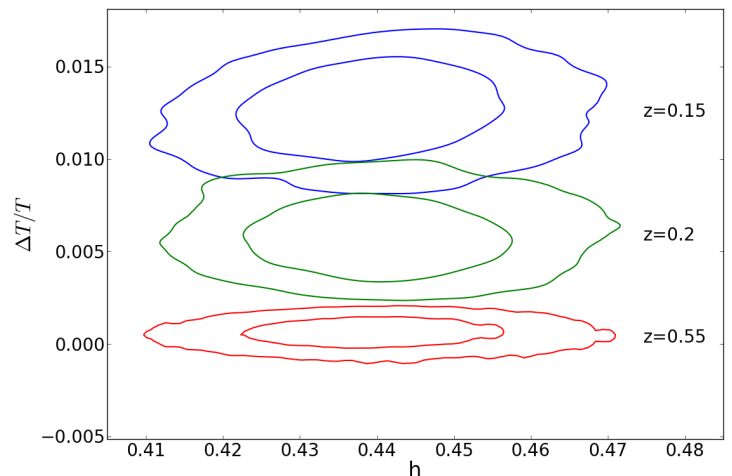

FIG. 8: The 68% and 95% likelihood contours in the space of $\Delta T/T$ and $H_0 = 100h$ kms^{-1}Mpc^{-1}, for off-center observers at $z = 0.15$, 0.20 and 0.55, for the MCMC sample constrained by SN+CMB+H_0+kSZ data. The $\Delta T/T$ are much lower than for the MCMC sample in Fig. 7, but the Hubble rate is too low to be considered consistent with observations.
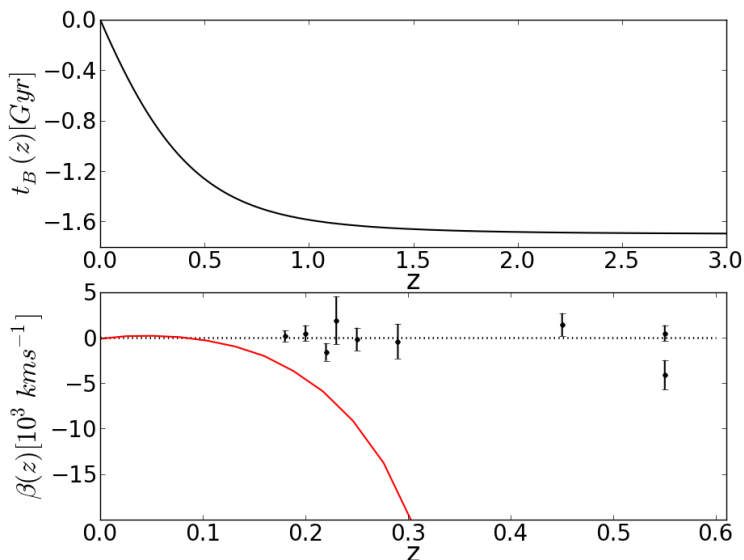
FIG. 9: Upper panel: Bang time function, $t_B(r)$, of the LTB model found in [8] which reproduces the Hubble rate, $H(z)$, and luminosity distance, $d_L(z)$, of ΛCDM. Lower panel: Velocity with respect to frame in which the CMB is isotropic, $\beta(z)$, for the same LTB model. $|\beta(z)|$ rapidly becomes very large ($\beta \approx -c$ for $z \gtrsim 0.6$), and produces a very poor fit to the kSZ data.

z (see Section II B), which almost always result in large $\Delta T/T$ because z_{in} and z_{out} in Eq. 14 differ significantly. As such, this model is also strongly disfavored by current kSZ data (see Fig. 9).

In fact, for large fluctuations in the bang time function we expect that there will *always* be a large dipole seen by off-center observers at some range of redshifts, corresponding to lines of sight that pass near to regions with a non-zero bang time gradient [68]. It therefore appears that one cannot simultaneously fit the supernova, CMB, H_0 and kSZ observations with a single LTB model unless one is prepared to violate one or more of the assumptions made in Section I.

V. DISCUSSION

In order to rigorously establish that $\Lambda \neq 0$, and that the concordance model of cosmology is correct, a model is required within which observations can be interpreted. The homogeneity and isotropy of the Universe on large scales is often assumed, and most analyses are performed using the highly symmetric FLRW solutions of general relativity. These are not the only viable ways to model the Universe, however, and recent advances in observational cosmology allow us to empirically test alternatives rather than relying on assumed symmetries of space-time on the largest scales. In this paper we used the spherically-symmetric, dust-only Lemaître-Tolman-Bondi (LTB) class of general relativis-

tic cosmological models, in their full generality, to test the radial homogeneity of the Universe on large scales. In particular, we consider the magnitude of the kinematic Sunyaev-Zel'dovich (kSZ) effect, which measures the dipole anisotropy of the CMB through a shift in the spectrum of CMB photons reflected from hot gas in clusters of galaxies. The kSZ effect is sensitive to large-scale inhomogeneity, as observers inhabiting an inhomogeneous universe would generically expect to see large anisotropies on their CMB skies.

In Section II, we introduced the theoretical framework for specifying these models and calculating observables in them. We defined a simple parametrization of the LTB radial function $k(r)$ that governs radial inhomogeneity at late times, and the function $t_B(r)$ that governs it at early times. This has been used to investigate underdense 'voids' which have previously been shown to produce good fits to the supernova data. We have discussed potential problems with models that are inhomogeneous at early times (i.e. that have non-constant t_B), including the potential for disruptions around our observed surface of last scattering. In models with a positive radial derivative of the bang time, $t'_B > 0$, it is found that shell crossing singularities form at early times, which pushes the surface of last scattering to later times. In models with negative bang time gradient, $t'_B < 0$, regions with a negative radial Hubble rate, $H_2 < 0$, form and the distance-redshift relation, $r(z)$, ceases to be monotonic. These features have observable effects that ultimately lead to predictions of a large CMB dipole anisotropy at low redshifts.

In Section III we reviewed some of the observational constraints that can be imposed on void models with constant bang time. Three key sets of observables were considered: The distance moduli of supernovae, the small-angle CMB power spectrum plus local Hubble rate, and upper limits on the magnitude of the kSZ effect for individual clusters of galaxies. Voids can fit the supernova data easily, but are unable to fit recent measurements of the CMB and H_0 simultaneously (they predict a value of H_0 that is far too low). Similarly, voids which fit the supernova data predict a large CMB dipole at redshifts up to $z \sim 1$, which is inconsistent with current kSZ measurements.

In Section IV we considered the effect on these constraints of allowing the bang time to vary. This resulted in a significant increase in the freedom of the models, and allowed the supernovae and CMB+H_0 data sets to be fit simultaneously, even with our simple parametrization of the LTB radial functions. Models with small kSZ signals, consistent with the data, were also found, but these required more complex profiles and gave worse fits to the supernova data. We then proceeded to combine all of the observational constraints, and found that voids which are able to fit the supernovae, CMB and H_0 predict an extremely large kSZ effect which is orders of magnitude greater than the measured upper limits. A joint fit to the supernova, CMB, H_0, and kSZ data with a signif-

icantly more complicated bang time profile also failed to produce good agreement with the data.

We also argued that any void model with a significant bang time inhomogeneity will produce a large kSZ effect at *some* redshift. Given that a varying bang time is necessary to resolve the low-H_0 problem, it seems that the combination of supernovae, CMB+H_0 and kSZ data is enough to effectively rule out LTB void models that attempt to explain cosmological data without dark energy, subject to the assumptions made in Section I. This goes some way toward demonstrating the homogeneity of the Universe on large scales.

We used the dipole approximation to calculate the magnitude of the kSZ effect in our models, but this only holds if the dipole term dominates the anisotropy of an off-center observer's sky [19, 29]. Otherwise, higher multipoles become important, and the dipole approximation overestimates the kSZ effect. The dipole will dominate as long as most lines of sight on the observer's sky pass through the void, as will be the case if the observer is firmly inside it, for example. For the models in Section IV C and IV D, and the Célérier *et al.* model in Section IV E, the inhomogeneity extends out to $z \geq 2$, and so the dipole approximation will always be a good one for observers at $z < 0.6$, where the kSZ data lie. The models with more complicated bang time profiles considered in Section IV E have much narrower inhomogeneities, however, and so we would expect the dipole approximation to be worse. These models predict low kSZ magnitudes and are close to being consistent with the kSZ data, so any overestimate due to the dipole approximation will have little effect on their total χ^2, which is anyway dominated by the poor fits to the supernova, CMB and H_0 data. We therefore conclude that the dipole approximation is sufficient for our purposes.

As we have tried to make clear throughout, our results are subject to several caveats that are summarized in Section I. The first, that we are exactly in the center of a perfectly spherically symmetric void, serves to simplify our calculations but is clearly unrealistic as it fails to take into account angular variations in, for example, the galaxy distribution. This could affect observables such as the dipole anisotropy of the CMB seen by off-center observers, potentially weakening the constraints we have derived using the kSZ effect. Considering ourselves as off-center observers [19, 52] and introducing linear perturbations [30, 53] would produce more realistic models and allow more observational data to be used (e.g. the matter power spectrum) at the expense of a significant increase in complexity. A better understanding of linear perturbations would also go some way toward addressing our second caveat, that the formation of the last scattering surface must be in an approximately-FLRW region. In general, one could expect features such as the coupling of scalar and tensor modes in LTB perturbations to produce secondary effects such as large B-mode polarizations [30]. This type of effect is completely absent in linear perturbation theory about FLRW backgrounds.

A particular limitation of LTB solutions as cosmological models is that they contain only dust, and cease to be applicable when radiation becomes important. If we want to approximate the Universe as an LTB model at late times, we must therefore match it to an appropriate solution containing radiation at early times. Solutions involving separate inhomogeneous matter and radiation fluids [31], spatially-varying physical quantities such as the photon-baryon ratio [14], and scale-dependent initial power spectra [32] have been considered, and serve to give some idea of the extra freedom that might be obtained in more general models. Specifically, altering the location and properties of the surface of last scattering can have a profound effect on the predicted kSZ signal [14] and the observed CMB [31, 32], and if one is prepared to consider this additional freedom, then our present results should not be expected to hold.

Finally, let us consider LTB models in the context of general inhomogeneity. Rather than allowing space-time to be described by a single LTB metric, it has been suggested that the LTB geometry could be used as an effective geometry to model the scale dependence of inhomogeneity after some averaging procedure has been applied to the fine-grained structure of the actual inhomogeneous geometry of the real Universe [54]. This is a considerable departure from the situation we have been considering here. In particular, if other observers are able to construct similar effective spherically symmetric geometries about their own locations then we should no longer expect distant clusters to see a large dipole in their CMB sky. This would completely relax the constraints that can be imposed from observations of the kSZ effect.

Note added: A preprint by J.P. Zibin [61] discussing the effect of bang time fluctuations on another tracer of anisotropy in voids, Compton y-distortion, appeared shortly after the original version of this paper was released. Its conclusions are in broad agreement with those presented here: Fluctuations in the bang time that are large enough to have a significant effect on the geometry of the Universe at late times (and thus have any bearing on the low-H_0 problem) would result in Compton y-distortions many times larger that can be reconciled with current observational constraints.

[1] Perlmutter, S. *et. al.*, *Astrophys. J.* **517**, 565 (1999).
[2] Riess, A. *et. al.*, *Astron. J.* **116**, 1009 (1998).
[3] Weinberg, S., *Rev. Mod. Phys.* **61**, 1 (1989).
[4] Lemaître, G., *Ann. Soc. Sci. Brussels* **A53**, 51 (1933) (reprinted in *Gen. Rel. Grav.* **29**, 641 (1997)).
[5] Tolman, R. C., *Proc. Nat. Acad. Sci. USA* **20**, 169 (1934) (reprinted in *Gen. Rel. Grav.* **29**, 935 (1997)).
[6] Bondi, H., *Mon. Not. Roy. Astron. Soc.* **107**, 410 (1947).
[7] Célérier, M-N. & Schneider, J., *Phys. Lett.* **A249**, 37 (1998).
[8] Célérier, M-N., Bolejko, K. & Krasiński, A., *Astron. Astrophys.* **518** A21 (2010).
[9] Biswas, T., Notari, A. & Valkenburg, W., *JCAP* **1011**, 030 (2010).
[10] Bolejko, K., Célérier, M-N. & Krasiński, A., *arXiv:1102.1449* (2011).
[11] Bolejko, K. & Wyithe, J., *JCAP* **0902**, 020 (2009).
[12] Clifton, T., Ferreira, P. G. & Land, K., *Phys. Rev. Lett.* **101**, 131302 (2008).
[13] García-Bellido, J. & Haugbølle, T., *JCAP* **04**, 003 (2008).
[14] Yoo, C-M., Nakao, K. & Sasaki, M., *JCAP* **07**, 012 (2010).
[15] Zhang, P. & Stebbins, A., *arXiv:1009.3967* (2010).
[16] Zibin, J. P. & Moss, A., *arXiv:1105.0909* (2011).
[17] Moss, A., Zibin, J. P. & Scott, D., *Phys. Rev.* **D83**, 103515 (2011).
[18] Yoo, C-M., Nakao, K. & Sasaki, M., *JCAP* **10**, 011 (2010).
[19] Alnes, H. & Amarzguioui, M., *Phys. Rev.* **D74**, 103520 (2006).
[20] Clifton, T., Ferreira, P. G. & Zuntz, J., *JCAP* **07**, 029 (2009).
[21] Zibin, J. P., Moss, A. & Scott, D., *Phys. Rev. Lett.* **101**, 251303 (2008).
[22] Sunyaev, R. A. & Zeldovich, Y. B., *Mon. Not. Roy. Astron. Soc.* **190**, 413 (1980).
[23] Holzapfel, W. L. *et al.*, *Astrophys. J.* **481**, 35 (1997).
[24] Benson, B. A. *et al.*, *Astrophys. J.* **592**, 674 (2003).
[25] Kitayama, T. *et al.*, *Publ. Astron. Soc. Jap.* **56**, 17 (2004).
[26] Sudeep, D. *et al.*, *Astrophys. J.* **729**, 62 (2011); Dunkley, J. *et al.*, *arXiv:1009.0866* (2010).
[27] Hall, N. R. *et al.*, *Astrophys. J.* **718**, 632 (2010); Shirokoff, E. *et al.*, *Astrophys. J.* **736**, 61 (2011).
[28] Goodman, J., *Phys. Rev.* **D52**, 1821 (1995).
[29] García-Bellido, J. & Haugbølle, T., *JCAP* **09**, 016 (2008).
[30] Clarkson, C., Clifton, T. & February, S., *JCAP* **06**, 025 (2009).
[31] Clarkson, C. & Regis, M., *JCAP* **02**, 013 (2011).
[32] Nadathur, S. & Sarkar, S., *Phys. Rev.* **D83**, 063506 (2011).
[33] Zecca, A., *Nouvo Cim.* **B106**, 413 (1991).
[34] Etherington, I. M. H., *Phil. Mag.* **15**, 761 (1933) (reprinted in *Gen. Rel. Grav.* **39**, 1047 (2006)).
[35] Silk, J., *Astron. Astrophys.* **59**, 53 (1977).
[36] Hellaby, C. & Lake, K., *Astrophys. J.* **290**, 381 (1985).
[37] Sussman, R. A., *Class. Quant. Grav.* **27**, 175001 (2010).
[38] Hellaby, C. & Lake, K., *Astrophys. J.* **282**, 1 (1984).

[39] Linde, A., Linde, D. & Mezhlumian, A., *Phys. Lett. B* **345**, 203 (1995).
[40] Afshordi, N., Slosar, A. & Wang, Y., *JCAP* **01**, 019 (2011).
[41] Mustapha, N., Hellaby, C. & Ellis, G. F. R., *Mon. Not. Roy. Astron. Soc.* **292**, 817 (1997).
[42] February, S., Larena, J., Smith, M. & Clarkson, C., *Mon. Not. Roy. Astron. Soc.* **405**, 2231 (2010).
[43] Riess, A. G. *et al.*, *Ap. J* **730**, 119 (2011).
[44] Clifton, T. & Zuntz, J., *Mon. Not. Roy. Astron. Soc.* **400**, 2185 (2009).
[45] Komatsu, E. *et al.*, *Ap. J. Supp.* **192** 192, 18 (2011).
[46] Amanullah, R. *et al.*, *Astrophys. J.* **716**, 712 (2010).
[47] Wang, Y. & Mukherjee, P., *Phys. Rev.* **D76**, 103533 (2007).
[48] Vonlanthen, M., Räsänen, S. & Durrer, R., *JCAP* **08**, 023 (2010).
[49] Hu, W., Fukugita, M., Zaldarriaga, M. & Tegmark, M., *Astrophys. J.* **549**, 669 (2001).
[50] Lewis, A. & Bridle, S., *Phys. Rev.* **D66**, 103511 (2002).
[51] Jarosik, N., *et. al.*, *Ap. J. Supp.* **192**, 14 (2011).
[52] Foreman, S., Moss, A., Zibin, J. P. & Scott, D., *Phys. Rev.* **D82**, 103532 (2010).
[53] Zibin, J. P., *Phys. Rev.* **D78**, 043504 (2008).
[54] Célérier, M-N., *arXiv:1108.1373* (2011).
[55] Kashlinsky, A. *et al.*, *Astrophys. J.* **712**, L81 (2010).
[56] Kashlinsky, A. *et al.*, *Astrophys. J.* **732**, 1 (2011).
[57] Atrio-Barandela, F. *et al.*, *Astrophys. J.* **719**, 77 (2010).
[58] Osborne, S. J. *et al.*, *Astrophys. J.* **737**, 98 (2011).
[59] Song, Y-S. *et al.*, *JCAP* **1001**, 025 (2010).
[60] Marra, V. & Pääkkönen, M., *arXiv:1105.6099* (2011).
[61] Zibin, J. P., *arXiv:1108.3068* (2011).
[62] A detection of the kSZ effect is claimed in [55, 56], but see also [57–59].
[63] There are some subtleties with the sign of a_2 when $k > 0$. For details of this see [37].
[64] Our MCMC code is available at `http://www.physics.ox.ac.uk/users/bullp`.
[65] At least five pieces of information are required for a full, relatively model-independent specification of the CMB power spectrum [48], but in what follows we will choose to marginalize over (or fix) the overall normalization of the power spectrum and the spectral index of the initial scalar power spectrum, as these quantities are not important for constraining the large-scale structure that we are interested in here.
[66] Allowing z_* to be free would add an extra nuisance parameter to be fitted for in our MCMC runs, which would inevitably loosen the resulting constraints. As such, the CMB constraints we derive here should be considered to be conservative.
[67] Modifying the form of the initial power spectrum can significantly weaken CMB constraints on void models [32].
[68] While the model in Fig. 5 can be seen to fit current kSZ data, these data only extend out to $z \sim 0.6$. Even this model will have a large $\beta(z)$ for some $z > 0.6$.